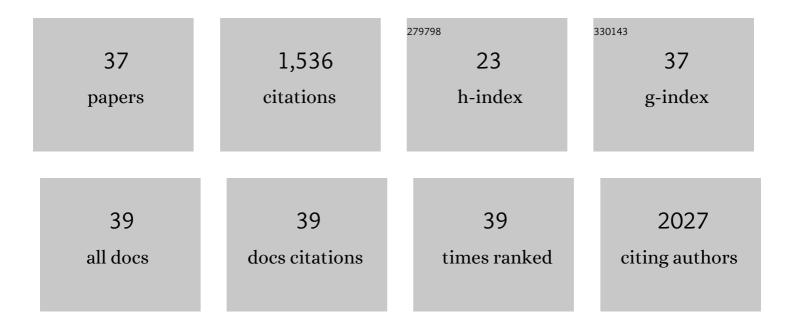
Shan-Shan Li

List of Publications by Year in descending order

Source: https://exaly.com/author-pdf/6867511/publications.pdf Version: 2024-02-01



SHAN-SHAN LI

#	Article	IF	CITATIONS
1	Engineering Co2+/Co3+ redox activity of Ni-mediated porous Co3O4 nanosheets for superior Hg(II) electrochemical sensing: Insight into the effect of valence change cycle and oxygen vacancy on electroanalysis. Sensors and Actuators B: Chemical, 2022, 354, 131095.	7.8	19
2	Hypersensitized electrochemical detection of Hg(II) based on tunable sulfur-doped porous Co3O4 nanosheets: Promotion Co2+/Co3+ valence change cycle and adsorption via introducing S. Chemical Engineering Journal, 2022, 435, 134950.	12.7	26
3	Sensitive detection of As(III) on Fe3O4/MoS2 through interfacial engineering to accelerate the Fe2+/Fe3+ cycle: Identifying the dominant role of electron transfer induced by valence change in synergistic electroanalysis. Sensors and Actuators B: Chemical, 2022, 366, 132022.	7.8	16
4	Hollow aluminosilicate microspheres with increased surface hydroxyl groups by etching method for electrochemical detection of Hg(II). Microchemical Journal, 2022, 180, 107610.	4.5	1
5	Oxygen vacancy enhanced Co3O4/ZnO nanocomposite with small sized and loose structure for sensitive electroanalysis of Hg(II) in subsidence area water. Sensors and Actuators B: Chemical, 2021, 326, 128967.	7.8	26
6	Zero-valent iron nanomaterial Fe ⁰ @Fe ₂ MnO ₄ for ultrasensitive electroanalysis of As(<scp>iii</scp>): Fe ⁰ influenced surficial redox potential. Chemical Communications, 2021, 57, 1324-1327.	4.1	9
7	Cobalt encapsulated in bamboo-like N-doped carbon nanotubes for highly sensitive electroanalysis of Pb(<scp>ii</scp>): enhancement based on adsorption and catalysis. Analytical Methods, 2021, 13, 2147-2156.	2.7	8
8	An ultra-sensitive electrochemical sensor of Ni/Fe-LDH toward nitrobenzene with the assistance of surface functionalization engineering. Talanta, 2021, 225, 122087.	5.5	29
9	Engineering surface electron and active site at electrochemical sensing interface of CN vacancy-mediated Prussian blue analogue for analysis of heavy metal ions. Applied Surface Science, 2021, 564, 150131.	6.1	11
10	Interlayer expanded nickel-iron layered double hydroxide by intercalation with sodium dodecyl sulfate for enhanced oxygen evolution reaction. Journal of Alloys and Compounds, 2021, 882, 160752.	5.5	27
11	Superior conductivity FeSe2 for highly sensitive electrochemical detection of p-nitrophenol and o-nitrophenol based on synergistic effect of adsorption and catalysis. Sensors and Actuators B: Chemical, 2021, 348, 130692.	7.8	20
12	Engineering multi-shell Mn-Co oxide for ultrasensitive electroanalysis of Pb(II) in mining subsidence area water with promotion of adsorption and electron mediation: Behaviors and mechanisms of Mn(II)/Mn(III) and Co(II)/Co(III) cycles. Electrochimica Acta, 2020, 360, 136991.	5.2	10
13	Crystal phase determined Fe active sites on Fe2O3 (γ- and α-Fe2O3) yolk-shell microspheres and their phase dependent electrocatalytic oxygen evolution reaction. Applied Surface Science, 2020, 533, 147368.	6.1	26
14	Changing the Blood Test: Accurate Determination of Mercury(II) in One Microliter of Blood Using Oriented ZnO Nanobelt Array Film Solutionâ€Gated Transistor Chips. Small, 2019, 15, e1902433.	10.0	9
15	Synergistic catalysis of N vacancies and â ⁻¹ 45 nm Au nanoparticles promoted the highly sensitive electrochemical determination of lead(<scp>ii</scp>) using an Au/N-deficient-C ₃ N ₄ nanocomposite. Environmental Science: Nano, 2019, 6, 1895-1908.	4.3	32
16	Surface Fe(II)/Fe(III) Cycle Promoted Ultra-Highly Sensitive Electrochemical Sensing of Arsenic(III) with Dumbbell-Like Au/Fe ₃ O ₄ Nanoparticles. Analytical Chemistry, 2018, 90, 4569-4577.	6.5	105
17	High Electrochemical Sensitivity of TiO _{2–<i>x</i>} Nanosheets and an Electron-Induced Mutual Interference Effect toward Heavy Metal Ions Demonstrated Using X-ray Absorption Fine Structure Spectra. Analytical Chemistry, 2018, 90, 4328-4337.	6.5	52
18	Noble-Metal-Free Co _{0.6} Fe _{2.4} O ₄ Nanocubes Self-Assembly Monolayer for Highly Sensitive Electrochemical Detection of As(III) Based on Surface Defects. Analytical Chemistry, 2018, 90, 1263-1272.	6.5	66

SHAN-SHAN LI

#	Article	IF	CITATIONS
19	Sensitive and interference-free electrochemical determination of Pb(II) in wastewater using porous Ce-Zr oxide nanospheres. Sensors and Actuators B: Chemical, 2018, 257, 1009-1020.	7.8	46
20	The selective capture of Pb ²⁺ in rice phloem sap using glutathione-functionalized gold nanoparticles/multi-walled carbon nanotubes: enhancing anti-interference electrochemical detection. Environmental Science: Nano, 2018, 5, 2761-2771.	4.3	12
21	Insights into diverse performance for the electroanalysis of Pb(II) on Fe2O3 nanorods and hollow nanocubes: Toward analysis of adsorption sites. Electrochimica Acta, 2018, 288, 42-51.	5.2	34
22	Electrochemical spectral methods for trace detection of heavy metals: A review. TrAC - Trends in Analytical Chemistry, 2018, 106, 139-150.	11.4	66
23	Defect- and phase-engineering of Mn-mediated MoS ₂ nanosheets for ultrahigh electrochemical sensing of heavy metal ions: chemical interaction-driven <i>in situ</i> catalytic redox reactions. Chemical Communications, 2018, 54, 9329-9332.	4.1	51
24	Electrochemically etched gold wire microelectrode for the determination of inorganic arsenic. Electrochimica Acta, 2017, 231, 238-246.	5.2	21
25	In Situ Underwater Laser-Induced Breakdown Spectroscopy Analysis for Trace Cr(VI) in Aqueous Solution Supported by Electrosorption Enrichment and a Gas-Assisted Localized Liquid Discharge Apparatus. Analytical Chemistry, 2017, 89, 5557-5564.	6.5	35
26	Competitive adsorption behavior toward metal ions on nano-Fe/Mg/Ni ternary layered double hydroxide proved by XPS: Evidence of selective and sensitive detection of Pb(II). Journal of Hazardous Materials, 2017, 338, 1-10.	12.4	72
27	Shape dependent stripping behavior of Au nanoparticles toward arsenic detection: evidence of enhanced sensitivity on the Au (111) facet. RSC Advances, 2016, 6, 30337-30344.	3.6	20
28	Electrochemical laser induced breakdown spectroscopy for enhanced detection of Cd(II) without interference in rice on layer-by-layer assembly of graphene oxides. Electrochimica Acta, 2016, 216, 188-195.	5.2	24
29	An atomically thick titanium phosphate thin layer with enhancing electrochemical sensitivity toward Pb(<scp>ii</scp>). RSC Advances, 2016, 6, 72975-72984.	3.6	11
30	Iron Oxide with Different Crystal Phases (α- and γ-Fe ₂ O ₃) in Electroanalysis and Ultrasensitive and Selective Detection of Lead(II): An Advancing Approach Using XPS and EXAFS. Analytical Chemistry, 2016, 88, 906-914.	6.5	123
31	Adsorbent Assisted <i>in Situ</i> Electrocatalysis: An Ultra-Sensitive Detection of As(III) in Water at Fe ₃ O ₄ Nanosphere Densely Decorated with Au Nanoparticles. Analytical Chemistry, 2016, 88, 1154-1161.	6.5	90
32	Sensitive and selective electrochemical detection of heavy metal ions using amino-functionalized carbon microspheres. Journal of Electroanalytical Chemistry, 2016, 760, 143-150.	3.8	67
33	Flexible nitrogen-doped graphene/carbon nanotube/Co ₃ O ₄ paper and its oxygen reduction activity. Nanoscale, 2014, 6, 7534-7541.	5.6	75
34	MOLECULAR TEMPLATES FOR CONTROLLING AND ORDERING ORGANIC MOLECULES ON SOLID SURFACES. Nano, 2012, 07, 1230001.	1.0	3
35	Surface Confined Metallosupramolecular Architectures: Formation and Scanning Tunneling Microscopy Characterization. Accounts of Chemical Research, 2009, 42, 249-259.	15.6	172
36	Control of Supramolecular Rectangle Self-Assembly with a Molecular Template. Journal of the American Chemical Society, 2007, 129, 9268-9269.	13.7	83

#	Article	IF	CITATIONS
37	Time-Dependent Organization and Wettability of Decanethiol Self-Assembled Monolayer on Au(111) Investigated with STM. Journal of Physical Chemistry B, 2006, 110, 1794-1799.	2.6	39